JOURNAL OF VIROLOGY, July 2011, p. 6822–6831 Vol. 85, No. 14
0022-538X/11/$12.00 doi:10.1128/JVI.00510-11

Virally Expressed Interleukin-10 Ameliorates Acute Encephalomyelitis and Chronic Demyelination in Coronavirus-Infected Mice▽

Kathryn Trandem,[1] Qiushuang Jin,[2] Kayla A. Weiss,[1] Britnie R. James,[1] Jingxian Zhao,[2,3] and Stanley Perlman[2]*

Interdisciplinary Program in Immunology[1] and Department of Microbiology,[2] University of Iowa, Iowa City, Iowa 52242, and Institute for Tissue Transplantation and Immunology, Jinan University, Guangzhou 510630, China[3]

Received 14 March 2011/Accepted 9 May 2011

The absence of interleukin-10 (IL-10), a potent anti-inflammatory cytokine results in increased immune-mediated demyelination in mice infected with a neurotropic coronavirus (recombinant J2.2-V-1 [rJ2.2]). Here, we examined the therapeutic effects of increased levels of IL-10 at early times after infection by engineering a recombinant J2.2 virus to produce IL-10. We demonstrate that viral expression of IL-10, which occurs during the peak of virus replication and at the site of disease, enhanced survival and diminished morbidity in rJ2.2-infected wild-type B6 and IL-10$^{-/-}$ mice. The protective effects of increased IL-10 levels were associated with reductions in microglial activation, inflammatory cell infiltration into the brain, and proinflammatory cytokine and chemokine production. Additionally, IL-10 increased both the frequency and number of Foxp3^{+} regulatory CD4 T cells in the infected central nervous system. Most strikingly, the ameliorating effects of IL-10 produced during the first 5 days after infection were long acting, resulting in decreased demyelination during the resolution phase of the infection. Collectively, these results suggest that the pathogenic processes that result in demyelination are initiated early during infection and that they can be diminished by exogenous IL-10 delivered soon after disease onset. IL-10 functions by dampening the innate or very early T cell immune response. Further, they suggest that early treatment with IL-10 may be useful adjunct therapy in some types of viral encephalitis.

The anti-inflammatory cytokine interleukin-10 (IL-10) is a pleiotropic cytokine that is produced in abundant quantities during most parasitic, bacterial, viral, and fungal diseases. Until recently, IL-10 was believed to be most important during chronic infections with its expression linked to the development of chronic infections in mice such as those caused by *Leishmania major*, lymphocytic choriomeningitis virus (LCMV), and *Toxoplasma gondii* (3, 5, 12, 44). In these infections, abrogation of IL-10-mediated immunosuppression results in accelerated pathogen clearance, and this is sometimes accompanied by immunopathological disease. IL-10 has also been implicated in pathogen persistence in chronic human infections such as hepatitis C virus (HCV) and *Mycobacterium tuberculosis* (10, 16).

Only recently has a role for IL-10 in acute diseases been appreciated. In acute viral infections caused by pathogens such as influenza A virus (IAV), simian virus 5 (SV5), respiratory syncytial virus (RSV), and mouse hepatitis virus (MHV), IL-10 production is maximal at the height of the adaptive inflammatory response, with IL-10 expressed largely by virus-specific CD4 and CD8 T cells (27, 30, 36, 37, 39, 41). We and others showed that virus-specific IL-10^{+} CD8 T cells are more activated and cytolytic than are IL-10^{-} CD8 T cells responding to the same epitope (39, 41). IL-10 primarily acts to suppress macrophages and dendritic cell (DC) function by inhibiting expression of major histocompatibility complex (MHC) class II and costimulatory molecules such as CD80/CD86 and production of proinflammatory cytokines and chemokines, including IL-12 (31). IL-10 also has direct effects on T cells, inhibiting activation and cytokine expression. Production of IL-10 by highly activated virus-specific T cells raises the possibility that IL-10 functions via both autocrine and paracrine signaling to limit inflammation during acute phases of the disease. Nevertheless, the importance of IL-10's anti-inflammatory effects in acute disease is not firmly established, since it continues to be expressed during the resolution phases of an infection.

IL-10 diminished disease in mice infected with a variant of MHV, strain JHMV (J2.2-V-1) that causes mild acute encephalitis and chronic demyelinating encephalomyelitis (4, 38). Demyelination in these mice is largely mediated by the immune response (43, 45). Infection of IL-10$^{-/-}$ mice resulted in increased morbidity and mortality and augmented demyelination compared to wild-type mice (43, 45). To determine IL-10's role during the early stages of infection, we engineered recombinant J2.2-V-1 (rJ2.2) expressing IL-10 (rJ2.2-IL-10) or encoding a nonfunctional version of the gene (rJ2.2-ΔIL-10). Infection with rJ2.2-IL-10 resulted in expression of high levels of IL-10 at the site of infection, with levels that became undetectable as the virus was cleared. Since IL-10 has a half-life of approximately 2 h (26), cytokine levels track with virus clearance, making this a useful system for evaluating the role of exogenously added IL-10 during the peak phase of the infection. We show that early viral expression of IL-10 enhanced survival and diminished chronic demyelination in rJ2.2-infected B6 and IL-10$^{-/-}$ mice.

MATERIALS AND METHODS

Mice. Specific-pathogen-free, 6-week-old C57BL/6 (B6) mice were purchased from the National Cancer Institute (Bethesda, MD). IL-10$^{-/-}$ (B6.129P2-Il10tm1Cgn/J) mice were bred in the animal facility of the University of Iowa. After viral inoculation, mice were examined and weighed daily. Clinical evalua-

* Corresponding author. Mailing address: Department of Microbiology, BSB 3-730, University of Iowa, Iowa City, IA 52242. Phone: (319) 335-8549. Fax: (319) 335-9999: E-mail: Stanley-Perlman@uiowa.edu.

▽ Published ahead of print on 18 May 2011.

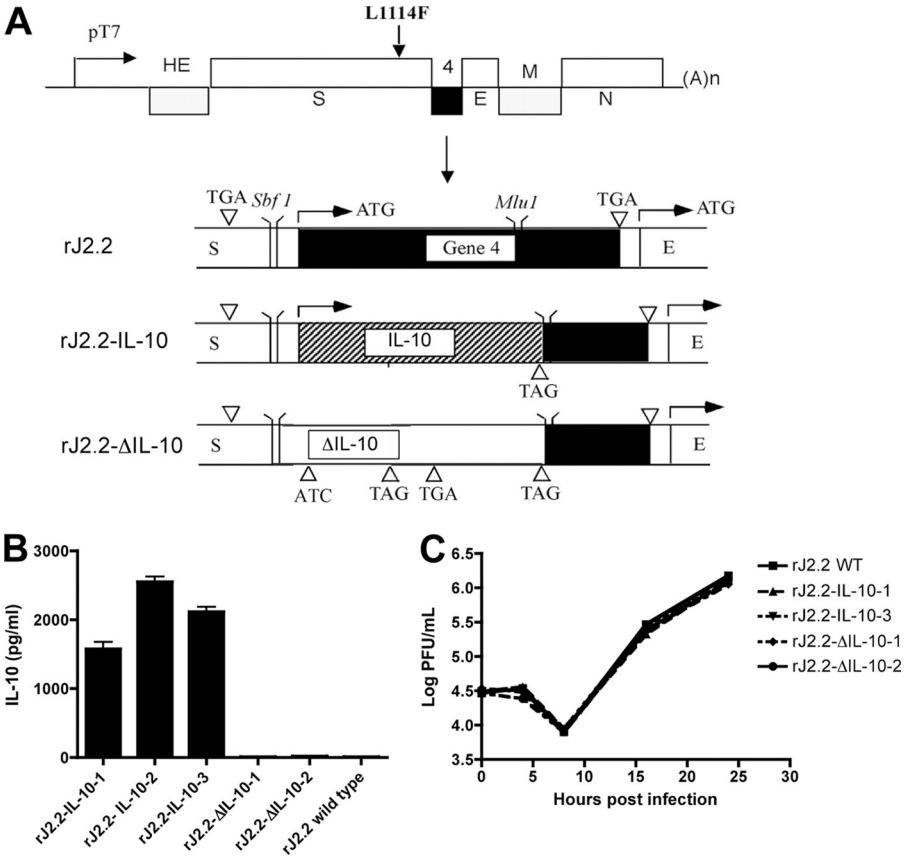

FIG. 1. Generation and expression of recombinant rJ2.2-IL-10 and rJ2.2-ΔIL-10. (A) Schematic diagram of rJ2.2-IL-10 and rJ2.2-ΔIL-10, showing the insertion of the IL-10 gene into gene 4 of rJ2.2 and a mutated initiation and two introduced stop codons in rJ2.2-ΔIL-10. Abbreviations: HE, hemagglutinin-esterase; S, surface; E, envelope; M, transmembrane; N, nucleocapsid. (B) 17Cl-1 cells were infected with wild-type (WT) rJ2.2, rJ2.2-IL-10, or rJ2.2-ΔIL-10, and 24 h later, supernatants were collected for measurement of IL-10 by ELISA. (C) 17Cl-1 cells were infected with rJ2.2, rJ2.2-IL-10, or rJ2.2-ΔIL-10 and harvested at various time points for viral titers. Data are from two independent experiments with 2 or 3 replicates/experiment.

tion was based on the following scoring system: 0, asymptomatic; 1, limp tail; 2, wobbly gait with righting difficulty; 3, hind limb weakness and extreme righting difficulty; 4, hind limb paralysis; 5, moribund. All animal studies were approved by the University of Iowa Animal Care and Use Committee.

Recombinant viruses. Targeted recombination was used to generate recombinant virus, as previously described (21, 29). We introduced the *Il10* gene, produced synthetically (GENEART, Burlingame, CA), into rJ2.2, replacing part of open reading frame 4 (ORF4) as described previously (Fig. 1A) (17, 18). Insertion of exogenous genetic material into ORF4 does not affect virulence (35). For a control, another construct was made in which the start codon (AT**G**) was mutated to AT**C** (boldface nucleotide changed), and Arg (**A**GA) and Gln (**C**AG) residues at positions 13 and 19 of the *Il10* gene were mutated to termination codons (**T**GA) and (**T**AG), respectively, using overlapping extension PCR (designated pJ2.2.ΔIL-10). Recombinant viruses were propagated, and the titers of the viruses were determined on 17Cl-1 and HeLa-MHVR cells, respectively (17, 18, 21, 35). Sequence analysis prior to use in further studies confirmed the presence of the introduced genes. To control for any unwanted mutations that might have occurred during the process of targeted recombination, multiple isolates of each virus were developed (three rJ2.2-IL-10 isolates and two rJ2.2-ΔIL-10 isolates). Identical results were obtained with the different isolates. Subsequently, most *in vivo* experiments used single isolates of rJ2.2-IL-10 and rJ2.2-ΔIL-10. Mice were inoculated intracerebrally (i.c.) with 1,000 or 500 PFU in 30 μl of Dulbecco modified Eagle medium (DMEM). To confirm retention of IL-10 or deletion of IL-10, RNA was analyzed by reverse transcription-PCR (RT-PCR) using virus-specific primers that flanked the inserted sequence, as described previously (17, 18). A 608-nucleotide product is expected if the insert is present.

Growth kinetics and expression of IL-10 in tissue culture. 17Cl-1 cells were infected with virus at a multiplicity of infection of 1 PFU per cell. Samples were harvested at the indicated times. Viral titers were determined on HeLa-MHVR cells, and IL-10 expression was determined by enzyme-linked immunosorbent assay (ELISA).

Antibodies and flow cytometric analyses. All antibodies were purchased from BD-Pharmingen (San Diego, CA) unless indicated otherwise below. Natural killer (NK) cells were $CD45^+$ $CD3^-$ $NK1.1^+$. Macrophages were $CD45^+$ $CD11b^+$ $Ly6C^+$ $Ly6G^-$. Neutrophils were $CD45^+$ $CD11b^+$ $Ly6C^+$ $Ly6G^+$. Microglia were $CD45^{int}$ $CD11b^+$. MHC class II was detected with fluorescein isothiocyanate (FITC)-conjugated anti-I-A/I-E antibodies from eBioscience (San Diego, CA). Microglial activation was assessed by measuring the expression of CD40 and CD80 (eBioscience) and CD86 (Biolegend, San Diego, CA). For detection of regulatory T cells (Tregs), cells were stained with peridinin chlorophyll protein (PerCP)-conjugated anti-CD4 monoclonal antibody (MAb). After permeabilization and fixation, cells were stained with phycoerythrin (PE)-conjugated anti-Foxp3 antibody or PE-conjugated isotype control rat IgG2a MAb as described by the manufacturer (eBiosciences). For detection of intracellular cytokine expression, CD8 or CD4 T cells were stimulated for 5 h with 1 μM peptide S510 (spanning residues S510 to 518 of the surface [S] glycoprotein) or 5 μM peptide M133 (spanning residues M133 to 147 of the transmembrane [M] protein) in the presence of 1 μl/ml Golgiplug (BD Pharmingen) and antigen-presenting cells (APCs) (CHB3 cells, $H\text{-}2D^b$, $I\text{-}A^b$). Intracellular gamma interferon (IFN-γ) and IL-10 expression was detected following fixation and permeabilization (BD Pharmingen). Cells were then incubated with anti-CD16/CD32-biotin and anti-CD4 or anti-CD8, followed by avidin-PerCP. Results are shown after gating on CD16/CD32-negative cell populations. Cells were analyzed using a FACSCalibur (BD Biosciences).

Preparation of central nervous system (CNS) mononuclear cells. Brain mononuclear cells were isolated as described previously (48). Briefly, tissue was dis-

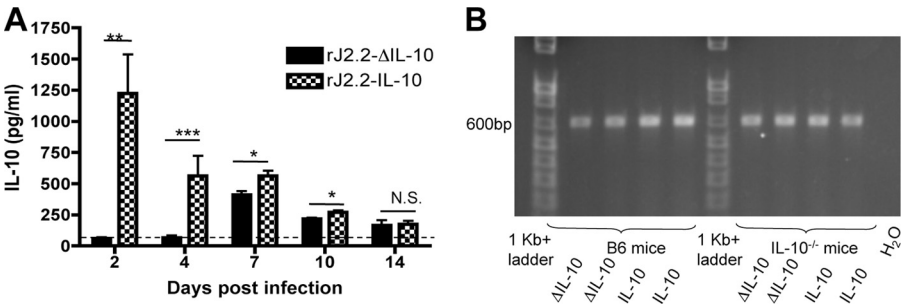

FIG. 2. Expression of virus gene-encoded IL-10 is stable in rJ2.2-IL-10-infected mice. (A and B) C57BL/6 (B6) (A and B) or IL-10$^{-/-}$ (B) mice were infected with rJ2.2-IL-10 or rJ2.2-ΔIL-10 and sacrificed at various times postinfection. IL-10 expression in the brain was confirmed by (A) ELISA and RT-PCR (B) as described in Materials and Methods. The broken line depicts the limit of detection. Statistical significance is indicated as follows: *, $P < 0.05$; **, $P < 0.01$; ***, $P < 0.001$; N.S., not significant. Data are from two independent experiments with ≥2 mice/group.

persed using 25-gauge needles, and digested with collagenase D (1 mg/ml; Roche Diagnostics) and DNase I (0.1 mg/ml; Roche Diagnostics) at 37°C for 30 min. Mononuclear cells were isolated by passing the tissue through a 70-μm cell strainer and centrifugation after resuspension in 30% Percoll (Pharmacia, Uppsala, Sweden).

ELISA. Brain tissue samples were homogenized directly into 50 mM Tris, 150 mM NaCl, 5 mM EDTA, 1 mM Na_3VO_4, 1% NP-40, and a protease inhibitor cocktail (Complete protease inhibitor cocktail; Roche, Mannheim, Germany) as described previously (40). IL-10, IL-6, tumor necrosis factor (TNF), and chemokine (C-C motif) ligand 2 (CCL2) ELISAs were performed using reagents and protocols provided by the manufacturer (eBioscience). Samples were plated in duplicate.

Quantification of demyelination. For examination of demyelination, 8-μm zinc formalin-fixed sections were stained with luxol fast blue (LFB) and counterstained with hematoxylin and eosin. Images of stained spinal cord sections were digitalized using an Optiphot charge-coupled camera attached to a Leitz diaplan light microscope (Leica Microsystems, Wetzlar, Germany). Quantification of demyelination was performed in a blind manner as previously described (46).

qRT-PCR. Brain RNA was extracted using TRIzol reagent (Invitrogen/Life Technologies, Carlsbad, CA) and reverse transcribed using Superscript II (Invitrogen) according to the manufacturer's instructions. Cytokine mRNA levels were quantified by quantitative reverse transcription-PCR (qRT-PCR) using SYBR green (SA Biosciences, Frederick, MD). The primers used for qRT-PCR were as follows: IL-10 F (F for forward), 5′-GCGTCGTGATTAGCGATGATG-3′; IL-10 R (R for reverse), 5′-CTCGAGCAAGTCTTTCAGTCC-3′; TNF F, 5′-TCAGCCGATTTGCTATCTCA-3′; TNF R, 5′-CGGACTCCGCAAAGTCTAAG-3′; CCL2 F, 5′-AGCACCAGCCAACTCTCACT-3′; CCL2 R, 5′-TCATTGGGATCATCTTGCTG-3′; IL-6 F, 5′-ACCACGGCCTTCCCTACTTC-3′; IL-6 R, 5′-CTCATTTCCACGATTTCCCAG-3′; chemokine (C-X-C motif) ligand 10 (CXCL10) F, 5′-AAGTGCTGCCGTCATTTTCT-3′; CXCL10 R, 5′-TTCATCGTGGCAATGATCTC-3′; hypoxanthine-guanine phosphoribosyltransferase (HPRT) F, 5′-GCGTCGTGATTAGCGATCATC-3′; HPRT R, 5′-CTCGAGCAAGTCTTTCAGTCC-3′. Amplification was performed using the Applied Biosystems 7300 sequence detector (Applied Biosystems, Foster City, CA). The specificity of amplification was confirmed using melting curve analysis. Data were analyzed as previously described (20), with normalization to HPRT.

Statistical analysis. Two-tailed unpaired Student's *t* tests were used to analyze differences in mean values between groups. A log rank sum test was used to analyze survival curves. All results are expressed as means ± standard errors of the means (SEM). Differences with *P* values of <0.05 were considered significant.

RESULTS

Generation and expression of IL-10-producing rJ2.2 virus. To test the effects of increasing IL-10 levels at early times postinfection (p.i.) and at the site of infection, we used reverse genetics to develop a rJ2.2 that expressed murine IL-10 (rJ2.2-IL-10) (Fig. 1A). For a control, we also engineered a virus encoding an IL-10 gene with a mutated start codon and two early stop codons (rJ2.2-ΔIL-10) (Fig. 1A). To confirm IL-10 expression, we infected murine fibroblast 17Cl-1 tissue culture cells with rJ2.2, three different isolates of rJ2.2-IL-10, or two isolates of rJ2.2-ΔIL-10. IL-10 mRNA was detected in cells infected with rJ2.2-IL-10 or rJ2.2-ΔIL-10 but not rJ2.2 (data not shown). Sequence analysis confirmed the presence of the full-length IL-10 gene in rJ2.2-IL-10-infected cells and a mutated IL-10 gene in the cells infected with rJ2.2-ΔIL-10. We then examined infected cell supernatants for IL-10 protein expression by ELISA at 24 h p.i. As shown in Fig. 1B, all rJ2.2-IL-10 isolates expressed similarly high levels of IL-10, while the rJ2.2-ΔIL-10 isolates and wild-type rJ2.2 produced no IL-10 protein. To determine whether insertion of IL-10 or ΔIL-10 affected virus replication, we examined the kinetics of virus growth in 17Cl-1 cells. rJ2.2-IL-10, rJ2.2-ΔIL-10, and rJ2.2 replicated with similar kinetics, demonstrating no effect of IL-10 expression on virus replication (Fig. 1C).

Exogenous IL-10 expression in rJ2.2-IL-10-infected B6 mice. In order to examine the expression of recombinant IL-10 *in vivo*, B6 mice were infected with 1,000 PFU of either rJ2.2-IL-10 or rJ2.2-ΔIL-10. Levels of infectious virus are maximal at days 3 to 5 p.i. in rJ2.2-infected B6 mice, with clearance occurring by day 14 p.i. (4). As seen in Fig. 2A, robust production of IL-10 protein was detected in the CNS of rJ2.2-IL-10-infected B6 mice. IL-10 levels were 10 fold higher in rJ2.2-IL-10-infected mice than in rJ2.2-ΔIL-10-infected mice at day 2 p.i., although the levels were very similar by day 7 p.i. By this time p.i., infectious virus is largely cleared and most IL-10 is derived from the host, with IL-10 levels similar to those reported previously (15, 41). Of note, serum IL-10 levels in all mice were below the limit of detection (32.0 pg/ml).

Exogenous genes inserted into recombinant mouse hepatitis virus are sometimes deleted during murine infection (9, 17). Therefore, we examined the brains of rJ2.2-IL-10- and rJ2.2-ΔIL-10-infected mice at day 7 p.i. by RT-PCR to assess retention of the IL-10 or ΔIL-10 gene. Only PCR products corresponding to intact IL-10 genes were detected (Fig. 2B), suggesting that significant deletion had not occurred and that IL-10 expression *in vivo* was stable for at least 7 days.

Virus gene-encoded IL-10 is protective in rJ2.2-infected B6 mice. Next, we determined whether IL-10 expressed in rJ2.2-IL-10-infected B6 mice diminished disease. As shown in Fig. 3A, rJ2.2-IL-10-infected B6 mice exhibited a slight increase in

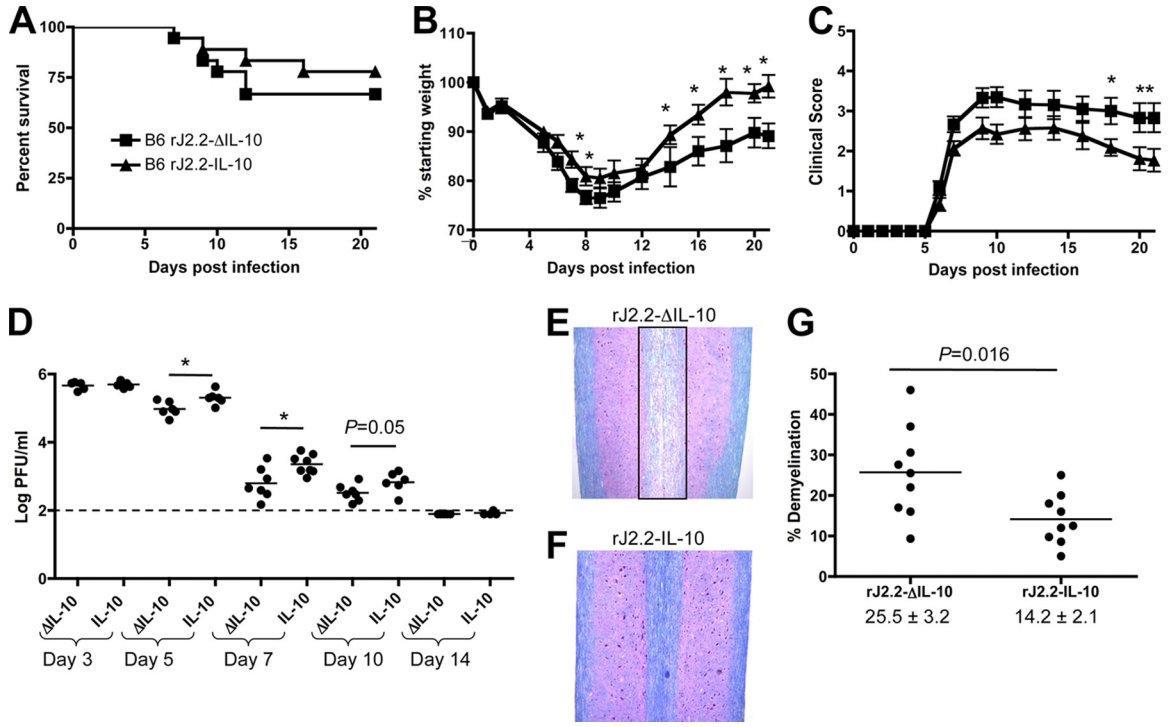

FIG. 3. B6 mice infected with rJ2.2-IL-10 have improved clinical outcomes and slower kinetics of virus clearance compared to rJ2.2-ΔIL-10-infected mice. (A to C) B6 mice were infected with 1,000 PFU of rJ2.2-IL-10 ($n = 19$) or rJ2.2-ΔIL-10 ($n = 19$) and examined for survival (A), weight (days 7 or 8 and 14 to 21, $P < 0.05$) (B), and clinical score (days 18 to 21, $P < 0.05$) (C) as described in Materials and Methods. (D) Virus titers were determined at the indicated times postinfection (p.i.). Each symbol represents the value for an individual mouse, and the mean of the group is shown by a short horizontal line. The broken line depicts the limit of detection. *, $P < 0.05$. (E and F) To detect demyelination, spinal cord sections were harvested at day 21 postinfection from B6 mice infected with rJ2.2-ΔIL-10 (E) or rJ2.2-IL-10 (F) and stained with luxol fast blue. (G) Percent demyelination from individual mice at day 21 postinfection. The numbers below the two groups in the graph are the mean percentages of demyelination ± SEM. Data are from two (D) or four (A to C and G) independent experiments with ≥3 mice/group.

survival compared to mice infected with rJ2.2-ΔIL-10, though this was not statistically significant. In contrast, weight loss and clinical scores were significantly reduced in rJ2.2-IL-10-infected B6 mice (Fig. 3B and C; weight loss, days 7 to 8 and 14 to 21, $P < 0.05$; clinical score, days 18 to 21, $P < 0.05$). However, this decrease in clinical disease in rJ2.2-IL-10-infected B6 mice was associated with diminished ability to control virus replication. Virus titers were significantly higher at days 5 and 7 p.i. in rJ2.2-IL-10-infected B6 mice than in rJ2.2-ΔIL-10-infected B6 mice, although differences diminished by day 10 p.i. (Fig. 3D). Virus was cleared from most mice by day 14 p.i.

Immunopathological disease in rJ2.2-infected mice is manifested by myelin destruction, which is maximal at 2 to 3 weeks after infection and occurs during the process of virus clearance (42). To determine whether increased IL-10 expression, by dampening the immune response, diminished myelin destruction, we examined infected spinal cords at day 21 p.i. The level of demyelination in rJ2.2-IL-10-infected mice was significantly decreased compared to those that were infected with rJ2.2-ΔIL-10 (Fig. 3E to G).

Inflammatory cell infiltration into the CNS is diminished while Treg frequency and numbers are increased in B6 mice infected with rJ2.2-IL-10. To explore the basis of diminished clinical disease and demyelination in rJ2.2-IL-10 mice, we initially compared the composition of the cellular infiltrates present in rJ2.2-IL-10- and rJ2.2-ΔIL-10-infected B6 mice (Fig. 4). At days 3 and 5 p.i., there was a significantly decreased number of macrophages and polymorphonuclear leukocytes (PMNs) in the CNS of B6 mice infected with rJ2.2-IL-10 compared to mice infected with rJ2.2-ΔIL-10 (Fig. 4B and C). The total numbers of CD4 and CD8 T cells were decreased at days 5 and 7 when mice infected with rJ2.2-IL-10 and rJ2.2-ΔIL-10 were compared, though only the difference in CD4 T cell numbers achieved statistical significance at day 5 p.i. (Fig. 4D and E).

To assess the effects of IL-10 expression on the numbers of virus-specific CD4 and CD8 T cells, we used intracellular cytokine staining for IFN-γ after stimulation with peptides corresponding to immunodominant CD4 (M133) and CD8 (S510) T cell epitopes. Lower numbers but not frequencies of M133-specific CD4 and S510-specific CD8 T cells were detected at day 7 after infection with rJ2.2-IL-10 compared to rJ2.2-ΔIL-10 (Fig. 4F and G), reflecting differences in the total numbers of infiltrating inflammatory cells.

IL-10 has a role in maintaining Treg function (34) and $Foxp3^+$ Tregs have important anti-inflammatory effects in rJ2.2-infected mice (40). To determine whether virus gene-encoded IL-10 enhanced the number of Tregs in the infected CNS, we examined the numbers and frequency of these cells at day 7 p.i. Both frequency and numbers of Tregs were increased in rJ2.2-IL-10-infected mice compared to those infected with rJ2.2-ΔIL-10, suggesting that IL-10 has both direct and indirect

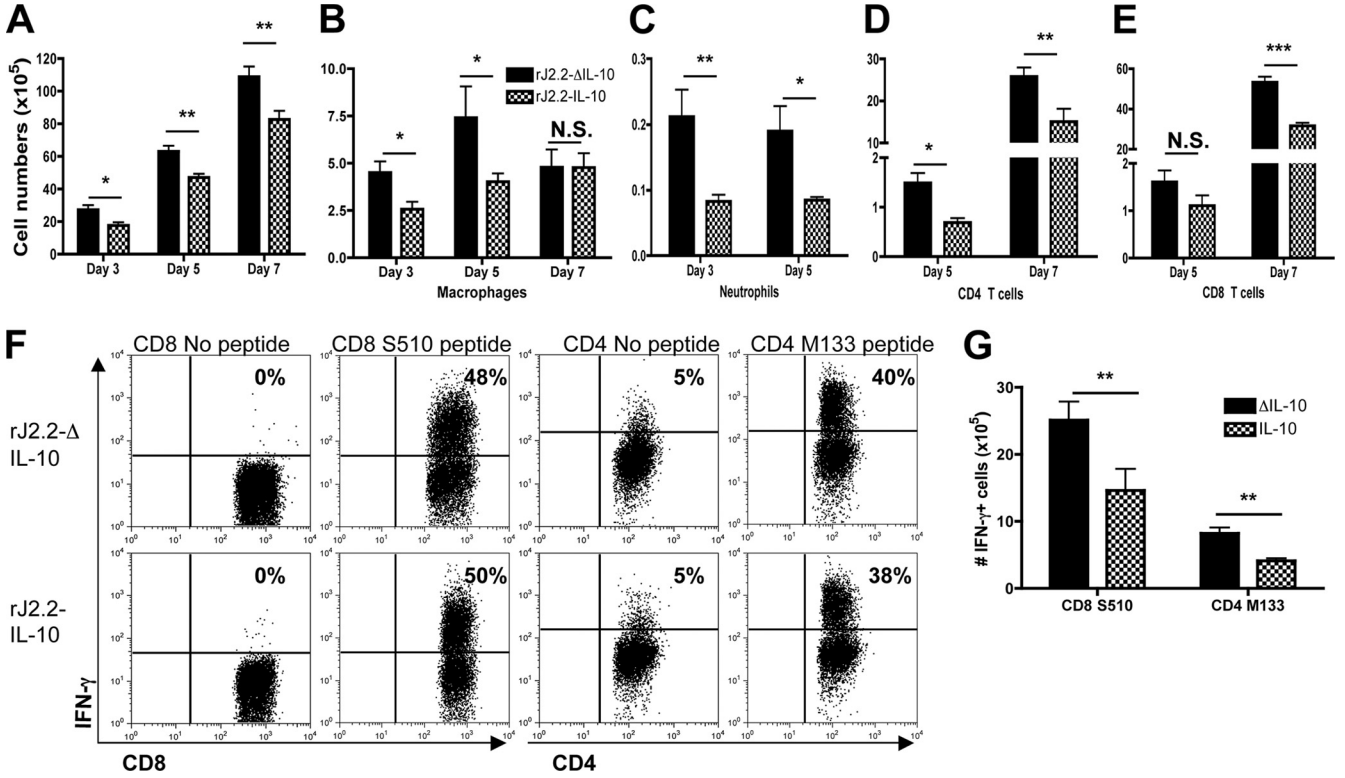

FIG. 4. B6 mice infected with rJ2.2-IL-10 have fewer infiltrating inflammatory cells than those infected with rJ2.2-ΔIL-10. Cells were harvested from the brains of B6 mice infected with rJ2.2-IL-10 (checkered bars) or rJ2.2-ΔIL-10 (black bars) at day 3, day 5, or day 7 postinfection. (A to E) Total numbers of infiltrating mononuclear cells (A), macrophages (B), neutrophils (C), CD4 T cells (D), and CD8 T cells (E) are shown. (F and G) Cells were harvested from infected mice at day 7 p.i. and examined directly *ex vivo* for IFN-γ expression after peptide stimulation. Plots are gated on $CD8^+$ or $CD4^+$ T cells. *, $P < 0.05$; **, $P < 0.01$; ***, $P < 0.001$; N.S., not significant. Data are from three independent experiments with ≥3 mice/group.

roles in enhancing the anti-inflammatory milieu in the CNS (Fig. 5).

IL-10 decreases microglial activation and proinflammatory cytokine and chemokine expression. Cellular infiltration into the infected CNS requires several factors, including activation of resident CNS cells, such as microglia and astrocytes, which present antigen and express proinflammatory cytokines and chemokines, such as CCL2 and TNF. Next, we examined microglia from rJ2.2-ΔIL-10- and rJ2.2-IL-10-infected B6 brains for evidence of activation. Virus expression of IL-10

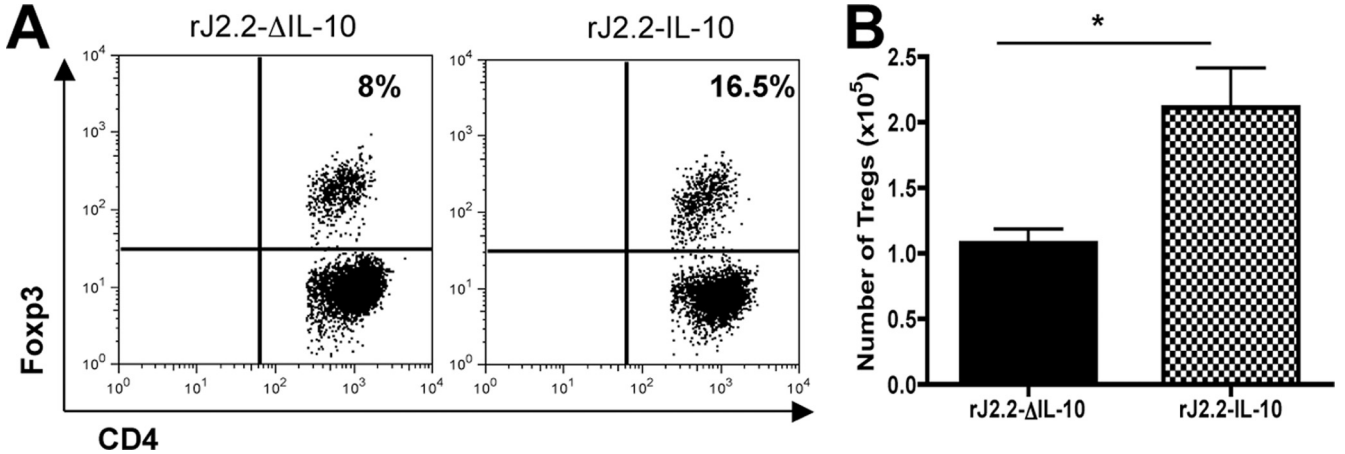

FIG. 5. rJ2.2-IL-10-infected B6 mice have increased frequency and number of Tregs in their CNSs compared with rJ2.2-ΔIL-10-infected B6 mice. Cells were harvested from the brains of B6 mice at day 7 p.i. (A) Flow cytometric plots of Foxp3 staining on gated CD4 T cells. (B) Total numbers of $Foxp3^+$ cells in B6 mice infected with rJ2.2-IL-10 or rJ2.2-ΔIL-10. *, $P < 0.05$. Data are representative of two independent experiments with ≥3 mice/group.

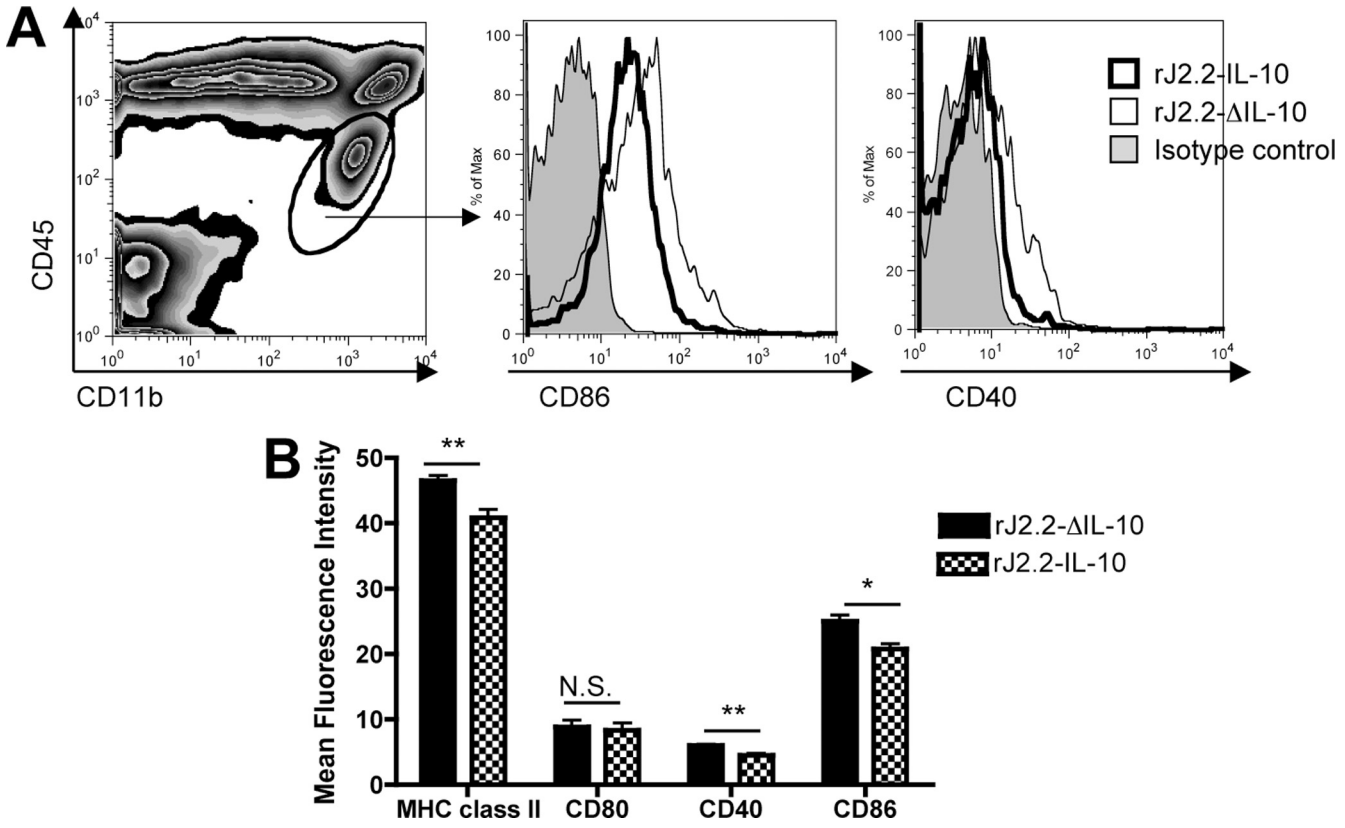

FIG. 6. Virus-encoded IL-10 suppresses microglia cell activation. Brain microglia harvested from rJ2.2-IL-10- or rJ2.2-ΔIL-10-infected B6 mice were examined for CD40, CD80, CD86, and MHC class II expression at day 5 p.i. (A) Microglia gating strategy is shown in the left-hand panel. The middle and right-hand panels show representative histograms of CD86 and CD40 staining (isotype control [filled], infected with rJ2.2-ΔIL-10 [light line], and infected with rJ2.2-IL-10 [thick black line]). (B) Mean fluorescence intensity of indicated molecules on microglia from B6 mice infected with rJ2.2-IL-10 (checkered bars) or rJ2.2-ΔIL-10. *, $P < 0.05$; **, $P < 0.01$; N.S., not significant. Data are representative of two independent experiments with ≥4 mice/group.

resulted in lower levels of expression of CD40, CD86, and MHC class II antigen on microglia (Fig. 6). Virus gene-encoded IL-10 expression also diminished the levels of several proinflammatory chemokines and cytokines in the brains of rJ2.2-IL-10-infected mice compared to rJ2.2-ΔIL-10-infected mice. At day 4 p.i., there were decreased mRNA levels of TNF, IL-6, CCL2, and CXCL10 in the brains of rJ2.2-IL-10-infected mice (Fig. 7A). Decreased mRNA levels corresponded to decreased protein levels of TNF, IL-6, and CCL2 as measured by ELISA (Fig. 7C). By day 10 p.i., no differences in brain chemokine or cytokine levels were detected (Fig. 7B). Concomitant with decreased cytokine/chemokine levels in the rJ2.2-IL-10-infected brain, the levels of TNF, CCL2, and IL-6 were statistically lower in draining cervical lymph nodes (CLN) at days 4 p.i. (Fig. 7D), with TNF mRNA levels remaining lower at day 10 p.i. (Fig. 7E).

Viral gene-encoded IL-10 is protective in rJ2.2-IL-10-infected IL-10$^{-/-}$ mice. B6 mice express IL-10 during both acute and chronic phases after rJ2.2 infection (41), and this host-derived IL-10 may act to enhance the effects of viral IL-10. To determine whether IL-10 expressed solely in the first few days after infection was sufficient for improved clinical outcomes and diminished demyelination, we infected IL-10$^{-/-}$ mice with 1,000 PFU of rJ2.2-IL-10 or rJ2.2-ΔIL-10. rJ2.2-IL-10-infected IL-10$^{-/-}$ mice had a significant increase in survival compared to mice infected with rJ2.2-ΔIL-10 ($P = 0.02$; Fig. 8A). The effects on survival were so dramatic, with few mice surviving, that all further studies in IL-10$^{-/-}$ mice were performed after infection with 500 PFU. IL-10$^{-/-}$ mice infected with this amount of rJ2.2-IL-10 had 100% survival (Fig. 8A) and significantly decreased weight loss (Fig. 8B, days 8 to 10 and 14 to 21, $P < 0.05$) and clinical scores (Fig. 8C, days 10 to 16, $P < 0.05$) compared to mice infected with rJ2.2-ΔIL-10.

IL-10 protein was detected in the brains of rJ2.2-IL-10-infected IL-10$^{-/-}$ mice until day 7 p.i., but by day 10 p.i., the levels were undetectable in most mice (Fig. 8D). This decrease in IL-10 expression reflected virus clearance, because as in infected B6 mice, IL-10 was not deleted from rJ2.2-IL-10- or rJ2.2-ΔIL-10-infected IL-10$^{-/-}$ mice by day 7 p.i. (Fig. 2B). Virus clearance was more rapid in rJ2.2-ΔIL-10-infected IL-10$^{-/-}$ mice than in mice infected with rJ2.2-IL-10 (Fig. 8E). In agreement with the results shown for infected B6 mice (Fig. 3E to G), the amount of demyelination in mice was significantly decreased in rJ2.2-IL-10-infected mice compared to that in mice infected with rJ2.2-ΔIL-10 (Fig. 8F). To further delineate the minimal time of expression required for an ameliorating effect, we blocked the IL-10 receptor (IL-10R) in IL-10$^{-/-}$

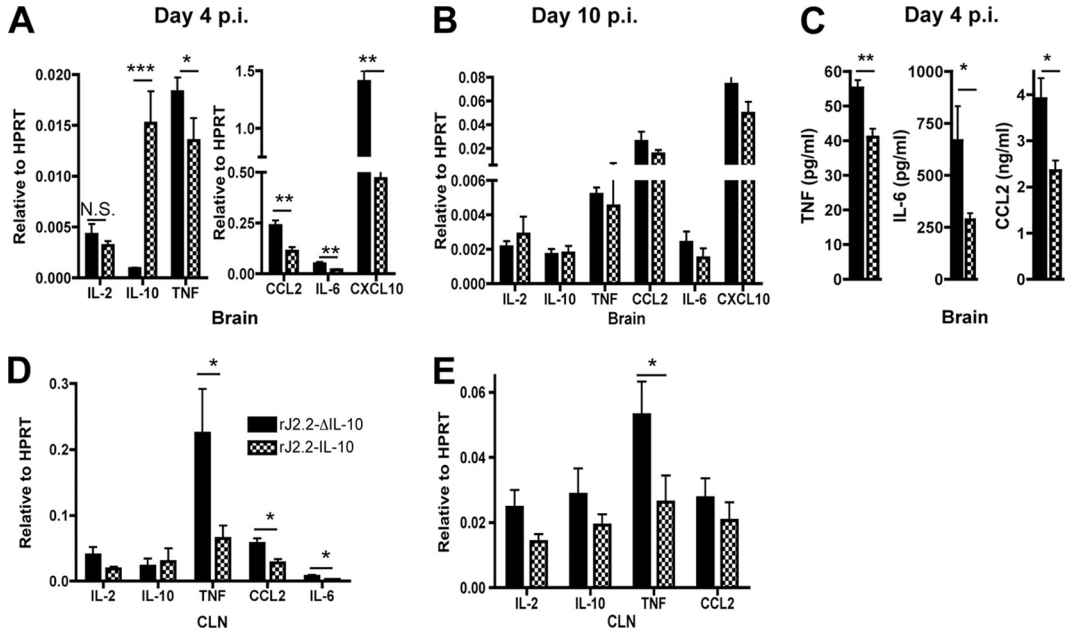

FIG. 7. Decreased production of proinflammatory cytokines and chemokines in the brains and cervical lymph nodes (CLN) of rJ2.2-IL-10-infected B6 mice compared to rJ2.2-ΔIL-10-infected B6 mice. (A to E) B6 mice were infected with rJ2.2-IL-10 (checkered bars) or rJ2.2-ΔIL-10 (black bars) and sacrificed at day 4 postinfection (p.i.) (A, C, and D) or day 10 p.i. (B and E) The levels of the indicated cytokines and chemokines in the brain (A to C) and CLN (D and E) were measured by qRT-PCR (A, B, D, and E) or ELISA (C) as described in Materials and Methods. *, $P < 0.05$; **, $P < 0.01$; ***, $P < 0.001$; N.S., not significant. Data are from two independent experiments with ≥3 mice/group.

mice beginning 1 day before or 5 days after infection with rJ2.2-IL-10. Other mice received isotype control antibody beginning 1 day prior to infection. Notably, antibody is able to penetrate the infected CNS as late as day 12 p.i. (28). IL-10R blockade prior to rJ2.2-IL-10 infection resulted in more severe clinical disease, weight loss, and demyelination than was observed in mice that received control antibody or anti-IL-10R antibody beginning at day 5 p.i. (Fig. 8G to J). Thus, IL-10 expression during only the first 5 days p.i. was sufficient to diminish evidence of myelin destruction 2 weeks later.

DISCUSSION

IL-10 is expressed maximally at early times p.i. in rJ2.2-infected mice (15, 41), yet many of its anti-inflammatory effects are manifested during the resolution phase of the infection. Here, using a recombinant rJ2.2 engineered to express IL-10, we show that IL-10 produced during the peak of virus replication results in improved outcomes and, more importantly, in diminished myelin destruction. Demyelination is first detected several days after virus clearance in rJ2.2-infected mice (42). Consequently, these results also indicate that the immunopathological process resulting in myelin destruction is actually initiated at early stages in the host inflammatory response. Further, the same degree of protection was evident in rJ2.2-IL-10-infected IL-$10^{-/-}$ mice, in which no IL-10 is made after infectious virus is cleared, confirming a critical role for IL-10 expressed at early times p.i. We demonstrated that virus-expressed IL-10 protected against weight loss, clinical disease, and mortality associated with rJ2.2-induced acute encephalomyelitis (Fig. 3 and 8). Neutralization of IL-10 activity beginning at day 5 p.i. in rJ2.2-IL-10-infected IL-$10^{-/-}$ mice did not enhance demyelination, suggesting that IL-10 functioned by diminishing the innate or very early T cell immune response. Consistent with this, the protective effect of enhanced IL-10 expression was associated with a dampened immune response, manifested by decreased levels of proinflammatory chemokines and cytokines (Fig. 7), decreased CNS infiltration of inflammatory cells (Fig. 4), diminished microglial activation (Fig. 6), and increased frequency and number of Tregs in the infected CNS (Fig. 5).

Virus-specific CD4 and CD8 T cells produce nearly all of the IL-10 detected in the rJ2.2-infected CNS at day 7 p.i. (42). The present study provides evidence, however, that the cellular source and timing of IL-10 production are not critical. T cells are not the source for virus-induced IL-10 because rJ2.2 infects oligodendrocytes, astrocytes, and microglia but not T cells (13). Additionally, T cells maximally produce IL-10 at day 7 p.i., while virus-induced IL-10 expression is maximal at day 2 p.i. Furthermore, T cell infiltration lags behind virus as it spreads in the CNS (42; S. Perlman, unpublished observations), suggesting that the exact location of IL-10 expression is not critical. Further, our results show that IL-10 does not have to be expressed for extended periods of time to have protective effects during both the acute and resolution phases of viral encephalitis.

The concept that exogenous IL-10 is useful therapeutically to diminish immunopathological disease has been previously examined in settings of transplantation and autoimmune disease (1, 32, 33). IL-10, delivered via adeno-associated virus or lentivirus vectors, diminishes the rate of graft rejection in several models of organ transplantation, including allogeneic

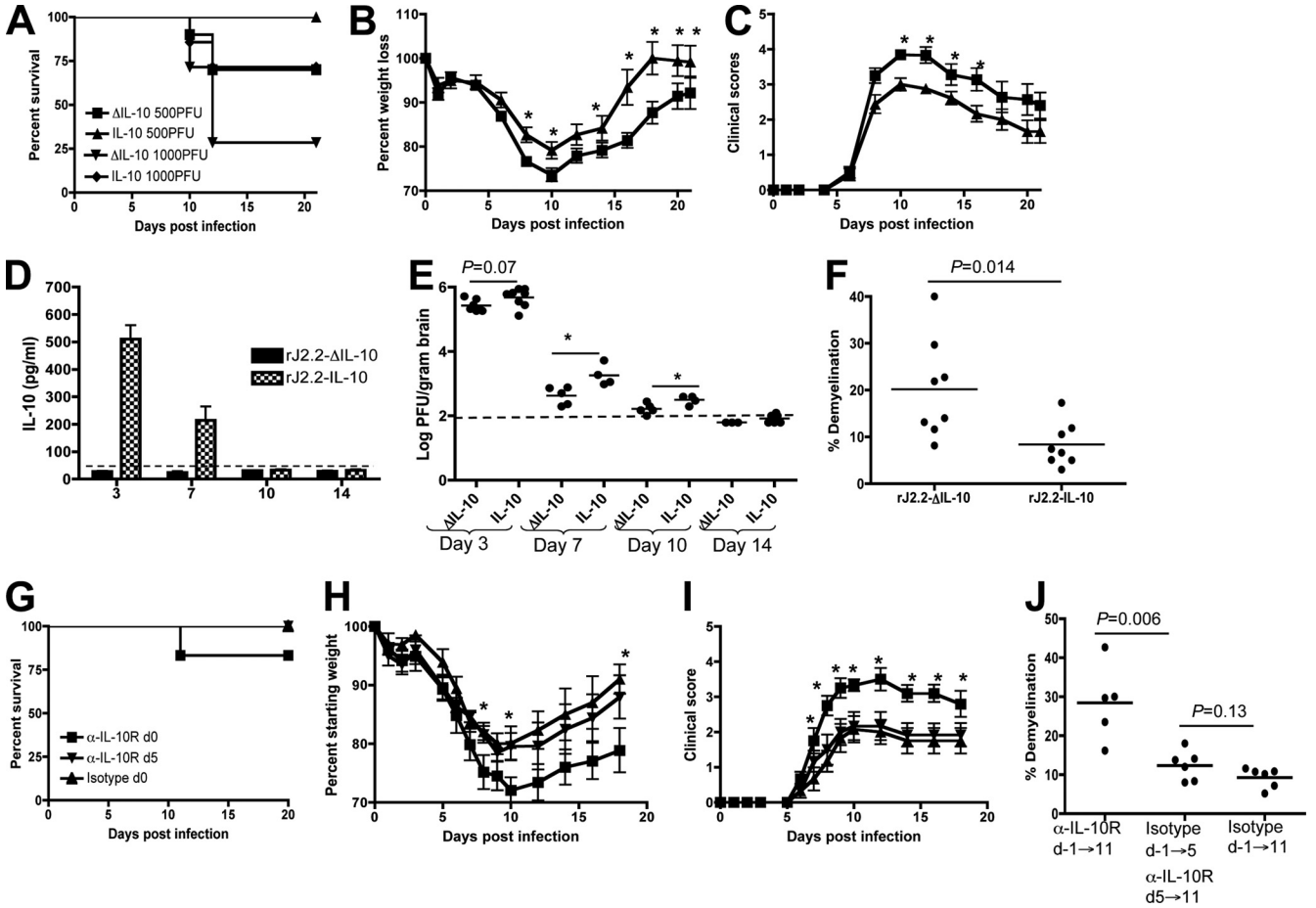

FIG. 8. IL-10$^{-/-}$ mice infected with rJ2.2-IL-10 have improved clinical outcomes with delayed viral clearance compared to rJ2.2-ΔIL-10-infected IL-10$^{-/-}$ mice. (A to C) IL-10$^{-/-}$ mice were infected with 500 PFU (A to I) (20 mice for each virus) or 1,000 PFU (20 mice for each virus) of rJ2.2-IL-10 or rJ2.2-ΔIL-10 (A) and examined for survival (A), weight loss (B), and clinical score (C). (D and E) IL-10 levels in brain homogenates (E) and virus titers in individual mice (E) were measured at the indicated times. The broken line depicts the limit of detection. (F) Percentage demyelination in individual mice at day 21 p.i. Data are from 2 independent experiments with ≥3 mice/group. (G to I) Mice received 500 μg anti-IL-10R (kindly provided by S. Varga, University of Iowa) (α-IL-10R, d-1→11) or isotype control MAb (isotype, d-1→11) on alternative days starting at 1 day prior to infection until 11 days postinfection. A third group received isotype control MAb on days −1, 1, and 3 and anti-10R MAb on days 5, 7, 9, and 11 p.i. (isotype, d-1→5, α-IL-10R, d5→11). Mice were examined for survival (G), weight loss (H), clinical scores (I), and demyelination (J). There were six mice in each group. *, $P < 0.05$.

heart, lung, liver, and pancreas transplants (8, 11, 19, 25). IL-10 diminished disease severity in several autoimmune diseases, including mice with experimental autoimmune encephalomyelitis (EAE) (6, 7, 24, 47).

Less is known about the effects of IL-10 treatment in virus infections. In the context of infection with vaccinia virus, exogenous IL-10 had small effects in immunocompetent mice, modestly decreasing NK and CD8 T cell function without affecting virus clearance or survival (22). In another study, IL-10 was administered intranasally to mice at the time of infection with respiratory syncytial virus (14). At 24 h p.i., significant reductions in lung pathology without effects on virus clearance were noted, although mice were not analyzed at later times p.i. Thus, exogenous IL-10 may be generally useful in virus infections, such as rJ2.2 and RSV, in which there is a substantial immunopathological component.

Although IL-10 is expressed directly at the site of rJ2.2 infection, we cannot rule out systemic effects of the virus-produced IL-10. rJ2.2 infection is confined to the CNS (13), and increased IL-10 levels were not observed in the serum (below the limit of detection of 32 pg/ml). However, we detected decreased levels of TNF and CCL2 mRNA in the draining CLN in rJ2.2-IL-10-infected mice compared to those in rJ2.2-ΔIL-10-infected mice (Fig. 7). These decreases may have resulted from systemic IL-10 spread (at levels in the blood beneath the level of detection) or may have been an indirect consequence of diminished inflammation in the brain. This diminished inflammatory response in the CLN may have contributed to an increased number of Tregs and diminished proinflammatory cellular infiltration into the brain (Fig. 4 and 5), amplifying the effects of the virus-produced IL-10.

In summary, we provide evidence that a relative paucity of IL-10 produced during a viral CNS infection contributes to more severe acute disease and immunopathology. The anti-

inflammatory immune response is likely to be required for disease resolution in all viral encephalitides, but the details of the response may be dependent on the pathogen. For example, regulatory T cells, rather than IL-10, appear to be most important for disease resolution in cases of West Nile virus encephalitis (2, 23). This may be related to the ability of rJ2.2 but not West Nile virus to cause demyelination. Thus, while our results suggest that IL-10 delivered early after infection may improve outcomes in some viral CNS infections, they also demonstrate the need to understand pathogen-specific encephalitis before instituting immune-modulating therapy.

ACKNOWLEDGMENTS

We thank Jincun Zhao for helpful discussions and critical review of the manuscript. We thank Steven Varga for providing anti-IL-10R antibody.

This work was supported by grants from the National Institute of Neurological Disorders and Stroke of the Public Health Service (NS-36592) and the National Multiple Sclerosis Society (RG-2864). K.T. was supported in part by an Institutional NRSA from the National Institutes of Health (AI007511-14).

REFERENCES

1. **Asadullah, K., W. Sterry, and H. D. Volk.** 2003. Interleukin-10 therapy–review of a new approach. Pharmacol. Rev. **55:**241–269.
2. **Bai, F., et al.** 2009. IL-10 signaling blockade controls murine West Nile virus infection. PLoS Pathog. **5:**e1000610.
3. **Belkaid, Y., et al.** 2001. The role of interleukin (IL)-10 in the persistence of Leishmania major in the skin after healing and the therapeutic potential of anti-IL-10 receptor antibody for sterile cure. J. Exp. Med. **194:** 1497–1506.
4. **Bergmann, C. C., T. E. Lane, and S. A. Stohlman.** 2006. Coronavirus infection of the central nervous system: host-virus stand-off. Nat. Rev. Microbiol. **4:**121–132.
5. **Brooks, D. G., et al.** 2006. Interleukin-10 determines viral clearance or persistence in vivo. Nat. Med. **12:**1301–1309.
6. **Choi, J. J., et al.** 2008. Mesenchymal stem cells overexpressing interleukin-10 attenuate collagen-induced arthritis in mice. Clin. Exp. Immunol. **153:**269–276.
7. **Croxford, J. L., M. Feldmann, Y. Chernajovsky, and D. Baker.** 2001. Different therapeutic outcomes in experimental allergic encephalomyelitis dependent upon the mode of delivery of IL-10: a comparison of the effects of protein, adenoviral or retroviral IL-10 delivery into the central nervous system. J. Immunol. **166:**4124–4130.
8. **Cypel, M., et al.** 2009. Functional repair of human donor lungs by IL-10 gene therapy. Sci. Transl. Med. **1:**4ra9.
9. **Das Sarma, J., E. Scheen, S. H. Seo, M. Koval, and S. R. Weiss.** 2002. Enhanced green fluorescent protein expression may be used to monitor murine coronavirus spread in vitro and in the mouse central nervous system. J. Neurovirol. **8:**381–391.
10. **de la Barrera, S., et al.** 2004. IL-10 down-regulates costimulatory molecules on Mycobacterium tuberculosis-pulsed macrophages and impairs the lytic activity of CD4 and CD8 CTL in tuberculosis patients. Clin. Exp. Immunol. **138:**128–138.
11. **Doenecke, A., E. Frank, M. N. Scherer, H. J. Schlitt, and E. K. Geissler.** 2008. Prolongation of heart allograft survival after long-term expression of soluble MHC class I antigens and vIL-10 in the liver by AAV-plasmid-mediated gene transfer. Langenbecks Arch. Surg. **393:**343–348.
12. **Ejrnaes, M., et al.** 2006. Resolution of a chronic viral infection after interleukin-10 receptor blockade. J. Exp. Med. **203:**2461–2472.
13. **Fleming, J. O., M. D. Trousdale, F. A. el-Zaatari, S. A. Stohlman, and L. P. Weiner.** 1986. Pathogenicity of antigenic variants of murine coronavirus JHM selected with monoclonal antibodies. J. Virol. **58:**869–875.
14. **Haeberle, H. A., et al.** 2004. IkappaB kinase is a critical regulator of chemokine expression and lung inflammation in respiratory syncytial virus infection. J. Virol. **78:**2232–2241.
15. **Kapil, P., et al.** 2009. Interleukin-12 (IL-12), but not IL-23, deficiency ameliorates viral encephalitis without affecting viral control. J. Virol. **83:**5978–5986.
16. **Kaplan, D. E., et al.** 2008. Peripheral virus-specific T-cell interleukin-10 responses develop early in acute hepatitis C infection and become dominant in chronic hepatitis. J. Hepatol. **48:**903–913.
17. **Kim, T. S., and S. Perlman.** 2003. Protection against CTL escape and clinical disease in a murine model of virus persistence. J. Immunol. **171:**2006–2013.
18. **Kim, T. S., and S. Perlman.** 2005. Viral expression of CCL2 is sufficient to induce demyelination in RAG1$^{-/-}$ mice infected with a neurotropic coronavirus. J. Virol. **79:**7113–7120.
19. **Kim, Y. H., et al.** 2008. Viral IL-10 gene transfer prolongs rat islet allograft survival. Cell Transplant. **17:**609–618.
20. **Kruse, N., M. Pette, K. Toyka, and P. Rieckmann.** 1997. Quantification of cytokine mRNA expression by RT PCR in samples of previously frozen blood. J. Immunol. Methods **210:**195–203.
21. **Kuo, L., G. J. Godeke, M. J. Raamsman, P. S. Masters, and P. J. Rottier.** 2000. Retargeting of coronavirus by substitution of the spike glycoprotein ectodomain: crossing the host cell species barrier. J. Virol. **74:**1393–1406.
22. **Kurilla, M. G., S. Swaminathan, R. M. Welsh, E. Kieff, and R. R. Brutkiewicz.** 1993. Effects of virally expressed interleukin-10 on vaccinia virus infection in mice. J. Virol. **67:**7623–7628.
23. **Lanteri, M. C., et al.** 2009. Tregs control the development of symptomatic West Nile virus infection in humans and mice. J. Clin. Invest. **119:**3266–3277.
24. **Lau, A. W., S. Biester, R. J. Cornall, and J. V. Forrester.** 2008. Lipopolysaccharide-activated IL-10-secreting dendritic cells suppress experimental autoimmune uveoretinitis by MHCII-dependent activation of CD62L-expressing regulatory T cells. J. Immunol. **180:**3889–3899.
25. **Li, J. Q., et al.** 2010. Induction of lymphocyte apoptosis in rat liver allograft by adenoviral gene transfection of human interleukin-10. Eur. Surg. Res. **44:**133–141.
26. **Li, L., J. F. Elliott, and T. R. Mosmann.** 1994. IL-10 inhibits cytokine production, vascular leakage, and swelling during T helper 1 cell-induced delayed-type hypersensitivity. J. Immunol. **153:**3967–3978.
27. **Lin, M. T., D. R. Hinton, B. Parra, S. A. Stohlman, and R. C. van der Veen.** 1998. The role of IL-10 in mouse hepatitis virus-induced demyelinating encephalomyelitis. Virology **245:**270–280.
28. **Liu, M. T., H. S. Keirstead, and T. E. Lane.** 2001. Neutralization of the chemokine CXCL10 reduces inflammatory cell invasion and demyelination and improves neurological function in a viral model of multiple sclerosis. J. Immunol. **167:**4091–4097.
29. **Masters, P. S.** 1999. Reverse genetics of the largest RNA viruses. Adv. Virus Res. **53:**245–264.
30. **McKinstry, K. K., et al.** 2009. IL-10 deficiency unleashes an influenza-specific Th17 response and enhances survival against high-dose challenge. J. Immunol. **182:**7353–7363.
31. **Mosser, D. M., and X. Zhang.** 2008. Interleukin-10: new perspectives on an old cytokine. Immunol. Rev. **226:**205–218.
32. **Mueller, C., et al.** 2009. The pros and cons of immunomodulatory IL-10 gene therapy with recombinant AAV in a Cftr$^{-/-}$-dependent allergy mouse model. Gene Ther. **16:**172–183.
33. **Muller, R. D., et al.** 2008. IL-10 overexpression differentially affects cartilage matrix gene expression in response to TNF-alpha in human articular chondrocytes in vitro. Cytokine **44:**377–385.
34. **Murai, M., et al.** 2009. Interleukin 10 acts on regulatory T cells to maintain expression of the transcription factor Foxp3 and suppressive function in mice with colitis. Nat. Immunol. **10:**1178–1184.
35. **Ontiveros, E., T. S. Kim, T. M. Gallagher, and S. Perlman.** 2003. Enhanced virulence mediated by the murine coronavirus, mouse hepatitis virus strain JHM, is associated with a glycine at residue 310 of the spike glycoprotein. J. Virol. **77:**10260–10269.
36. **Palmer, E. M., B. C. Holbrook, S. Arimilli, G. D. Parks, and M. A. Alexander-Miller.** 2010. IFNgamma-producing, virus-specific CD8+ effector cells acquire the ability to produce IL-10 as a result of entry into the infected lung environment. Virology **404:**225–230.
37. **Spender, L. C., T. Hussell, and P. J. Openshaw.** 1998. Abundant IFN-gamma production by local T cells in respiratory syncytial virus-induced eosinophilic lung disease. J. Gen. Virol. **79**(Part 7)**:**1751–1758.
38. **Stohlman, S. A., C. C. Bergmann, and S. Perlman.** 1998. Mouse hepatitis virus, p. 537–557. *In* R. Ahmed and I. Chen (ed.), Persistent viral infections. John Wiley & Sons, Ltd., New York, NY.
39. **Sun, J., R. Madan, C. L. Karp, and T. J. Braciale.** 2009. Effector T cells control lung inflammation during acute influenza virus infection by producing IL-10. Nat. Med. **15:**277–284.
40. **Trandem, K., D. Anghelina, J. Zhao, and S. Perlman.** 2010. Regulatory T cells inhibit T cell proliferation and decrease demyelination in mice chronically infected with a coronavirus. J. Immunol. **184:**4391–4400.
41. **Trandem, K., J. Zhao, E. Fleming, and S. Perlman.** 2011. Highly activated cytotoxic CD8 T cells express protective IL-10 at the peak of coronavirus-induced encephalitis. J. Immunol. **186:**3642–3652.
42. **Wang, F. I., D. R. Hinton, W. Gilmore, M. D. Trousdale, and J. O. Fleming.** 1992. Sequential infection of glial cells by the murine hepatitis virus JHM strain (MHV-4) leads to a characteristic distribution of demyelination. Lab. Invest. **66:**744–754.
43. **Wang, F. I., S. A. Stohlman, and J. O. Fleming.** 1990. Demyelination induced by murine hepatitis virus JHM strain (MHV-4) is immunologically mediated. J. Neuroimmunol. **30:**31–41.
44. **Wilson, E. H., U. Wille-Reece, F. Dzierszinski, and C. A. Hunter.** 2005. A critical role for IL-10 in limiting inflammation during toxoplasmic encephalitis. J. Neuroimmunol. **165:**63–74.
45. **Wu, G. F., A. A. Dandekar, L. Pewe, and S. Perlman.** 2000. CD4 and CD8 T

cells have redundant but not identical roles in virus-induced demyelination. J. Immunol. **165:**2278–2286.
46. **Xue, S., N. Sun, N. Van Rooijen, and S. Perlman.** 1999. Depletion of blood-borne macrophages does not reduce demyelination in mice infected with a neurotropic coronavirus. J. Virol. **73:**6327–6334.
47. **Yang, J., et al.** 2009. Adult neural stem cells expressing IL-10 confer potent immunomodulation and remyelination in experimental autoimmune encephalitis. J. Clin. Invest. **119:**3678–3691.
48. **Zhao, J., J. Zhao, and S. Perlman.** 2009. De novo recruitment of antigen-experienced and naive T cells contributes to the long-term maintenance of antiviral T cell populations in the persistently infected central nervous system. J. Immunol. **183:**5163–5170.